The distribution of the velocity and pressure fields in the nasal cavity at different respiration modes

Ya.V. Nosova¹, O.G. Avrunin¹, N.O. Shusliapina², O. Gryshkov³, B. Glasmacher³

¹Kharkiv National University of Radioelectronics, Nauki Avenue 14, Kharkiv, Ukraine

²Kharkiv National Medical University, Nauki Avenue 4, Kharkiv, Ukraine

³Institute for Multiphase Processes, Leibniz Universität Hannover, Callinstr. 36, Hannover, Germany

Contact: oleh.avrunin@nure.ua, gryshkov@imp.uni-hannover.de

Introduction

Topical are the problems associated with the prediction and evaluation of the functional results of endonasal surgery, which, in the case of respiratory and olfactory disorders [1-3], are the condition of air passage through the superior nasal passage and the restoration of olfactory sensitivity.

Changing the direction of the main air stream with nasal breathing leads to constant irritation of certain sections of the mucous membrane (for example, a portion of the mucosa of the nasal cavity that contains olfactory receptors, the so-called olfactory zone), which will subsequently lead to cellular infiltration in this region and then to hypertrophy of the mucosa shell. Therefore, it is necessary to study the distribution of velocities and pressures in the nasal cavity under different respiration regimes.

Materials and Methods

An important characteristic of nasal breathing is the distribution of air flow rates along the sections of the nasal cavity. When analyzing the existing approaches, it was determined that the main method of studying the aerodynamics of the nasal cavity is rhinomanometry. However, there is not always a clear correlation between anatomical and functional indicators, as well as subjective feelings of the patient and rhinomanometric data [4-9]. Numerical modeling of air passage through the nasal cavity is also used with the help of special applications that allow one to observe animated and static flow patterns on the computer screen, as well as integral air flow indicators, updated after each global iteration (changes in the flow structure as a function of time). The most famous and functional software packages are CFX (Canada, Great Britain, Germany), Ansys, Flotran module, (USA), STAR-CD (Great Britain), Fluent (USA), Numeca (Belgium), Flow-ER (Ukraine), Flow Vision (Russia).

Calculation of gas flow in modern software products is performed by numerically solving a system of equations describing the most general case of motion of a liquid medium. These are the Navier-Stokes equations and continuity. The boundary conditions, as a rule, are conditions for the flow velocity to be zero on the walls of the cavity, the distribution of velocity components in the input section and the zero of the first derivatives (in the direction of flow) of the velocity components in the outlet section, it is also possible to specify the average flow velocity or flow rate The output parameters are not specified. The pressure enters the equation only in the form of the first

derivatives, and its value is indicated only at one point in the computational domain. The most frequent phenomena in biological objects are turbulent currents. Direct simulation of turbulent flows by numerical solution of the Navier-Stokes equations written for instantaneous velocities is still extremely difficult, and, as a rule, not instantaneous, but averaged values of the velocities are of practical interest. Often, for the analysis of turbulent flows, instead of equations, the Reynolds equations and various models of turbulence are used.

The choice of the software package FlowVision for numerical modeling of aerodynamic processes in the nasal cavity is due to its availability in the Ukrainian software market, as well as the dissemination of its non-commercial versions (using an unlimited demo version of FlowVision 2 with a limited grid capacity of 15,000 cells).

However, the software product FlowVision does not have an embedded preprocessor (its own development tools for creating geometric objects), but it allows one to import the geometric configuration of the investigated structures (cavities) from many modern CAD-systems, for example, SolidWorks, Compass 3D, AutoCAD. Also, the package has a convenient interface that allows one to visualize the imported calculation area, specify the boundary conditions, environment properties, and the parameters to be examined. The FlowVision package uses a rectangular (Cartesian) design grid with the ability to adaptively select cell sizes and an approach to discretizing the equations of a mathematical model based on the finite volume method that provides the law of conservation of integral quantities (flow, momentum) in each of the computational grid cells. In this case, a certain closed region of gas flow is selected for which the fields of macroscopic quantities (for example, pressure drop, velocity, flow) are searched, describing the state of the medium in time and satisfying certain physical laws.

Convenient post-processing tools allow one to watch animated and static flow patterns on the screen, as well as integral flow indicators that are updated after each global iteration (changing the flow structure as a function of time). The set of available visualization tools includes standard two-dimensional graphics, vector fields, isolines and isosurfaces of the specified parameters, color filling of regions depending on the values of the parameter being studied, and animation of the motion of the fluid particles. After loading in the software package of the geometric model of the upper respiratory tract in * .STL format, the following parameters were specified:



- 1. Setting of the properties of the calculation area and parameters of the medium
- 2. Setting of boundary conditions (the value of the pressure differential on the nasal cavity (0.3, 1.0, 2.0, 5.0 and 10 kPa)
- 3. Introduction of flow through the nasal cavity (0.3, 0.6, 1, 2 and 4 s⁻¹), velocity at the wall equal to zero), type and additional parameters of the computational model.

Results

For a laminar regime in a section with radius a, we obtain a parabolic dependence of the velocities W on the distance from the center r:

$$W = 2W \left(1 - \frac{r^2}{a^2}\right) \tag{1}$$

where W is the average speed, r is the distance from the center, and a is the radius

For the turbulent regime, the velocity is defined as follows:

$$U = U_{max} \left(\frac{r}{a}\right)^{0.9\sqrt{\lambda}} \tag{2}$$

where U_{max} is the maximum speed, λ is the loss factor. Numerical data on the distribution of airflow velocities with an accuracy of 15% coincide with the analytical solutions obtained by equations (1, 2).

Whatever the law of velocity distribution in the section of the turbulent flow, the speed near the wall is 0, increasing to the axis of the flow. Consequently, there should be a low-speed layer, the thickness of which depends on Reynolds number *Re*, and the velocity increases from 0 to 90% of the velocity of the core of the flow (fig. 1) [4-6].

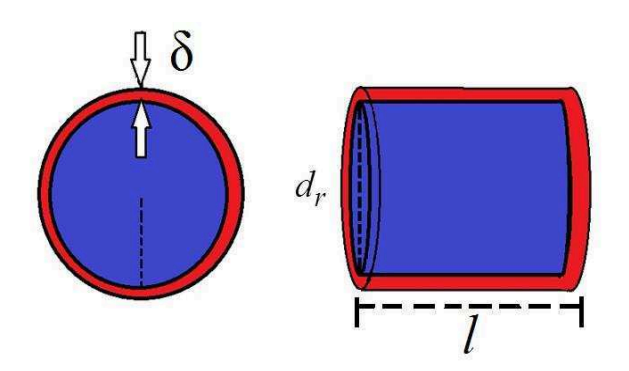


Figure 1: Schematic representation of the turbulent core of the stream (blue) and laminar boundary layer (red color) (d_r – is the hydraulic diameter, δ – the thickness of the laminar boundary layer, l –length of section)

With an increase in airflow velocity (with forced breathing-physical load, narrowing of the nasal passage), the thickness of the laminar boundary layer will decrease, the mucosa will be exposed to high-speed turbulent flow. Turbulization of the air flow will promote drying of individual areas of the mucous membrane of the nasal cavity, and as a result traumatization of the mucosa with subsequent morphological rearrangement of individual areas.

In the laminar regime, the highest velocity is observed in the central regions of the general and inferior nasal passages. In the turbulent regime, the velocity is also constant over a larger cross-sectional area and the velocity in the near-wall region is sharply reduced.

Air flow rates corresponded to 0.2, 1 and 2 L/s (calm, strengthened and forced - with physical exertion). The values of the distribution of the pressure difference were in the range 0.1-5 kPa - the upper limit characterizes the regime of forced breathing. The air flow rates were dependent on the nasal cavity sections in the range from 0.04 to 3 m/s, with maximum velocities observed in the nasal valve region and in the anatomical narrowing of the canal. With pronounced local resistances, the results of numerical simulation clearly showed areas of increased turbulence and swirl up to the reverse flow. These processes, leading to difficulty in nasal breathing, were clearly visualized with an aerodynamic drag coefficient greater than 1.5 kPa l/s.

The Reynolds numbers (fig. 2 c, d and fig. 3 c, d) depend essentially on the degree of forced breathing, and on the equivalent diameter and area of the nasal cavity and, in fact, mirror the distributions of the corresponding parameters. With quiet breathing (flow rate 0.5 l/s), the Reynolds numbers are small for almost all the cases under consideration (fig. 2 c, d and fig. 3 c, d) and sharply increase to 10,000 or more with forced respiration (at a flow rate of 2 l/s) and have extremes in generalized, or local narrowing of the nasal canals. Increased Reynolds numbers indicate an increase in turbulence in the corresponding areas of the nasal cavity.

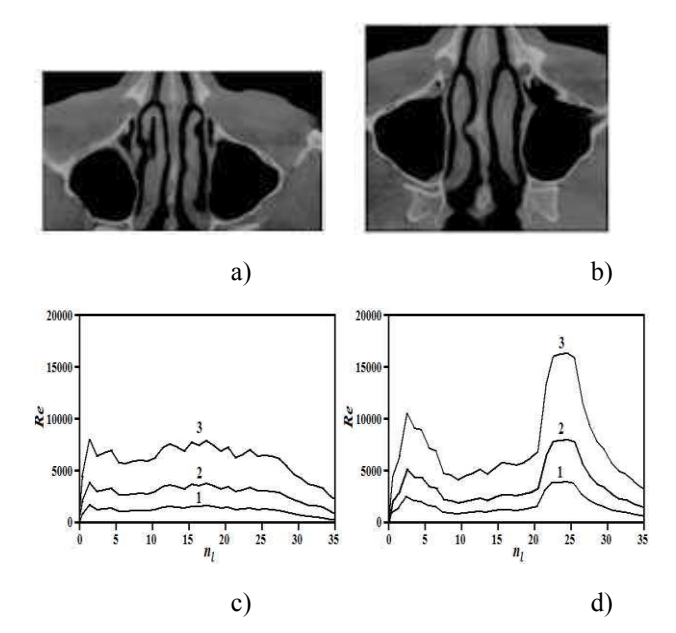


Figure 2: Images of characteristic axial SCT sections: a) without disturbance of nasal breathing; b) when the nasal septum is curved to the right; and the corresponding distributions for the right nasal passage: c), d) Reynolds numbers along the length of the nasal cavity at costs of 0.5 (1), 1.0 (2) and 2.0 (3) l/s (n - numbers of the frontal sections of the nasal cavity)



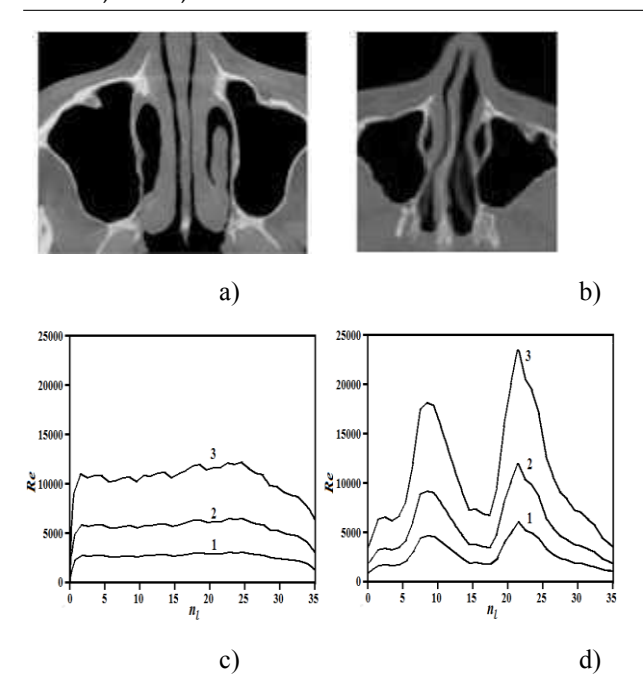


Figure 3: Images of characteristic axial SCT sections: a) in chronic rhinosinusitis, b) with S-shaped wavy curvature of the nasal septum; and the corresponding distributions for the right nasal passage c), d) of the Reynolds numbers along the length of the nasal cavity at flow rates of 0.5 (1), 1.0 (2) and 2.0 (3) 1/s (n - numbers of the frontal sections of the nasal cavity)

Discussion

Spatial mapping of the model of air passage through the nasal cavity, shown in fig. 4, allows one to visually estimate the air flow rate in the density of streamlines and in the animation mode to estimate the airflow velocity in different parts of the upper respiratory tract. The visualization of data on the pressure drop along the length of the nasal cavity is shown in fig. 5 - the pressure values will be constant across sections, which are isobaric planes. The errors of the averaged analytical and numerical method with respect to the calculation of the pressure in the sections of the nasal cavity are within 10%.

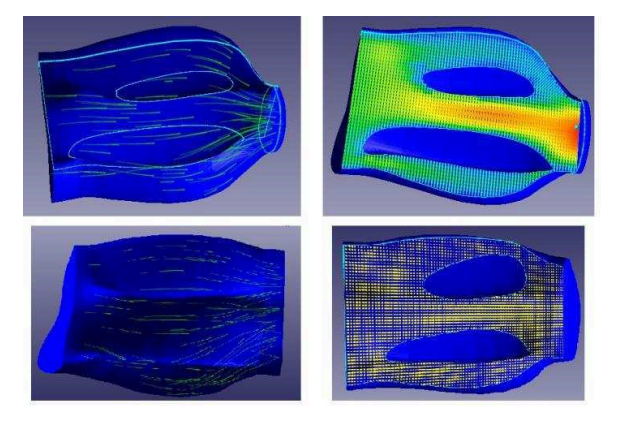


Figure 4: An illustration of the velocity field along the nasal passage (by the density of the airflow lines) from the data of the numerical experiment in the FlowVision package

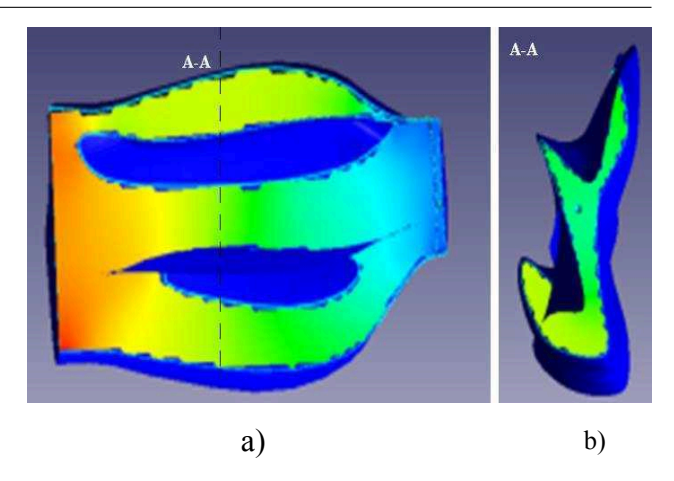


Figure 5: The distribution of pressure drop along the length of the nasal passage according to the data of the numerical experiment in the FlowVision package: a - along the sagittal section of the nasal passage; b - in one of the characteristic sections (AA) of the nasal passage (halftones illustrate the change in pressure drop)

Conclusions

Thus, the three-dimensional modeling of the air flow through the nasal cavity allows to map the nasal passages along the parameters studied and to study their local values, which is important for the planning of minimally invasive surgical interventions. However, the numerical modeling of the air flow in the nasal cavity with the help of software packages requires a large time (up to several working days), which is associated with a rather cumbersome stage of preparing the initial data. This includes interactive segmentation of anatomical objects, tracing contours of airborne structures, forming a three-dimensional model nasal moves and its subsequent loading into the simulation environment, eliminating model geometry errors, often resulting in repeated iterative implementation of the pre-stages and direct modeling stage, during which an aerodynamic and a large number of imaging parameters.

Analytical decisions are rather simplistic, but in most cases allow to adequately assessing the degree of nasal aerodynamics disturbance. In fact, this is an extended model of a one-dimensional flow of air in a channel in a complex form, in which the geometric characteristics of the nasal cavity are taken into account by the hydraulic diameter. Preparation for the construction and analysis of the numerical model is a much more labor-intensive process, but allows you to visualize detailed spatial patterns of the distribution of aerodynamic parameters (3d fields of velocities and pressure drops), which allows you to visualize reverse currents.

References

- [1] C. Manesse, C. Ferdenzi, M. Sabri, et al. Dysosmia-Associated Changes in Eating Behavior. Chem Percept, 10:104, 2017, doi:10.1007/s12078-017-9237-3
- [2] Nosova Ya., Avrunin O., Semenets V. Biotechnical system for integrated olfactometry diagnostics. Innovative technol-



- ogies and scientific solutions for industries, 1(1):64-68, 2017.
- [3] S. Boesveldt, S.T. Lindau, M.K. McClintock, T. Hummel, J.N. Lundström. Gustatory and olfactory dysfunction in older adults: a national probability study. Rhinology, 49(3): 324–330, 2011
- [4] I-C. Chen, Y-T. Lin, J-H. Hsu, Y-C. Liu, J-R. Wu, Z-K. Dai. Nasal Airflow Measured by Rhinomanometry Correlates with FeNO in Children with Asthma. PLoS ONE, 11(10): e0165440, 2016, doi: 10.1371/journal.pone.0165440
- [5] M. M. Tavakol, E. Ghahramani, O. Abouali, M. Yaghoubi, G. Ahmadi. Deposition fraction of ellipsoidal fibers in a model of human nasal cavity for laminar and turbulent flows. J Aerosol Sci, 113: 52-70, 2017
- [6] N. Curle. The Laminar Boundary Layer Equations. Courier Dover Publications, 176, 2017
- [7] J.-H. Lee. Y. Na, S.-K. Kim, S.-K. Chung. Unsteady flow characteristics through a human nasal airway. Respir Physiol Neurobiol 172(3): 136-146, 2010
- [8] O. Avrunin. Extended of diagnostic capabilities for the Rhinomanometry method. In O. Avrunin. N. Shuslyapina, J. Ivanchenko, 5.1: 315-321. Spatial aspects of socio-economic systems' development: the economy, education and health care. Monograph. Opole: The Academy of Management and Administration in Opole.- Publishing House WSZiA, 2015, ISBN 978-83-62683-64-0. 380.
- [9] Y. Nosova, N. Shushliapina, S.V. Kostishyn, L.G. Koval, Z. Omiotek, et al. The use of statistical characteristics of measured signals to increasing the reliability of the rhinomanometric diagnosis. Proc. SPIE 10031, Photonics Applications in Astronomy, Communications, Industry, and High-Energy Physics Experiments 2016, 100312M (September 28, 2016); doi:10.1117/12.2248364
- [10] H.F. Ismail, E. Osman, A.K. AL-Omari, O.G. Avrunin. The Role of Paranasal Sinuses in the Aerodynamics of the Nasal Cavities. International Journal of Life Science and Medical Research, 2(3): 52-55, 2012

Acknowledgements

The authors acknowledge the exchange program with East European Countries funded by DAAD (project number 54364768). We also thank Kalashnik M.V and the staff of the otorhinolaryngological department of the Kharkov regional hospital for assisting in experiments and validating the results.